

## Stable helical solitons in optical media

BORIS A MALOMED, G D PENG<sup>1</sup>, P L CHU<sup>1</sup>, ISAAC TOWERS<sup>2</sup>,  
ALEXANDER V BURYAK<sup>2</sup> and ROWLAND A SAMMUT<sup>2</sup>

Department of Interdisciplinary Studies, Faculty of Engineering, Tel Aviv University,  
Tel Aviv 69978, Israel

<sup>1</sup>Optical Communications Group, School of Electrical Engineering and Telecommunications,  
University of New South Wales, Sydney 2052, Australia

<sup>2</sup>School of Mathematics and Statistics, Australian Defence Force Academy, Canberra, ACT 2600,  
Australia

Email: malomed@eng.tau.ac.il

**Abstract.** We present a review of new results which suggest the existence of *fully stable* spinning solitons (self-supporting localised objects with an internal vorticity) in optical fibres with self-focusing Kerr (cubic) nonlinearity, and in bulk media featuring a combination of the cubic self-defocusing and quadratic nonlinearities. Their distinctive difference from other optical solitons with an internal vorticity, which were recently studied in various optical media, theoretically and also experimentally, is that all the spinning solitons considered thus far have been found to be *unstable* against azimuthal perturbations.

In the first part of the paper, we consider solitons in a nonlinear optical fibre in a region of parameters where the fibre carries exactly two distinct modes, viz., the fundamental one and the first-order *helical mode*. From the viewpoint of application to communication systems, this opens the way to doubling the number of channels carried by a fibre. Besides that, these solitons are objects of fundamental interest. To fully examine their stability, it is crucially important to consider collisions between them, and their collisions with fundamental solitons, in (ordinary or *hollow*) optical fibres. We introduce a system of coupled nonlinear Schrödinger equations for the fundamental and helical modes with nonstandard values of the cross-phase-modulation coupling constants, and show, in analytical and numerical forms, results of collisions between solitons carried by the two modes.

In the second part of the paper, we demonstrate that the interaction of the fundamental beam with its second harmonic in bulk media, in the presence of self-defocusing Kerr nonlinearity, gives rise to the first ever example of completely stable spatial ring-shaped solitons with intrinsic vorticity. The stability is demonstrated both by direct simulations and by analysis of linearized equations.

**Keywords.** Optical fibre; second harmonic generation.

**PACS Nos** 05.45.Y; 42.65.T; 42.81.D

### 1. Introduction

Solitons are self-supported localised packets, that can exist in various wave fields due to a balance between the tendency of the light packet to spread out under the action of dispersion (in the temporal domain) and/or diffraction (in the spatial domain), and the opposite tendency of the packet to self-focus under the action of the medium's nonlinearity. Solitons

in various optical media are especially interesting objects, due to both their fundamental importance and a great potential for application to optical communications. The most well-known example are solitons in optical fibres [1,2], that were theoretically predicted by Hasegawa and Tappert in 1973 and experimentally observed by Gordon, Mollenauer, and Tappert in 1980 (see a historical review in the book [2]). These solitons are expected to form the basis of a new generation of fibre-optic communication superhighways. In the development of optical communication lines with an extremely high bit-rate capacity wavelength-division-multiplexing (WDM) plays a crucial role. This technique assumes that a single fibre core may support many individual channels, each having its own carrier wavelength  $\lambda$  (with a separation  $\Delta\lambda \sim 0.5$  nm between adjacent channels). Searching for ways to further increase the number of channels carried by one fibre is the most important direction for further development of optical telecommunications.

Solitons in the optical fibre are, essentially, one-dimensional (1D) objects. A class of objects with less immediate opportunity for applications, but of paramount physical interest in their own right, are spatiotemporal solitons, i.e., fully localised objects moving at light velocity in 2D and 3D media, in which case they are also known as ‘light bullets’ (LBs) [3]. In the case of LBs, the most important issue is their stability, as ‘bullets’ in 2D and 3D media with the usual Kerr nonlinearity are definitely unstable because of the wave-collapse phenomenon [4]. The simplest way to possibly produce stable LBs, suggested long ago by Kanashov and Rubenchik [5], is to use a medium with a quadratic ( $\chi^{(2)}$ ) nonlinearity, which does not give rise to collapse in any physical dimension. Properties of the corresponding multidimensional solitons were studied in detail theoretically in works [6], using direct simulations and also a semi-analytical approach, based on the variational approximation. This was followed by experimental observation of *quasi*-2D solitons (which were localised in the longitudinal and one of two transverse directions, but delocalised in the other transverse direction) by Wise and his co-workers [7]. Thus far, truly 3D LBs have not yet been observed.

Once the existence of multidimensional optical solitons has been established, a challenging generalization is to consider spinning, or vortex, solitons in an anisotropic bulk medium. The internal vorticity inevitably creates a ‘hole’ inside the soliton, hence it will have the form of a ring (‘doughnut’). Spinning solitons may exist in both 2D and 3D. In fact, a 2D soliton with intrinsic vorticity may be construed either as a spinning 2D spatiotemporal soliton, or as a spatial soliton (with no time dependence) in the form of a spinning cylinder in a 3D medium, its cross section being an annulus due to the internal ‘hole’ induced by the vorticity. In the latter case, the corresponding spatial soliton is frequently described as (2+1)D.

Direct simulations of the spinning 2D solitons in  $\chi^{(2)}$  media (as well as in media with a saturable nonlinearity) have demonstrated that they, unlike their stable zero-spin counterparts, are subject to a strong instability against azimuthal perturbations that destroy the soliton’s rotational symmetry, and eventually split it into several fragments which fly out in tangential directions [8]. This instability was also confirmed by a direct experiment with (2+1)D solitons [9]. Fully 3D spinning solitons in  $\chi^{(2)}$  media can be found too, and they also turn out to be strongly unstable against azimuthal perturbations [10].

Another possibility is to consider a medium characterised by a combination of focusing cubic and defocusing quintic nonlinearity, which is known to be an adequate model for the so-called PTS optical crystal [11]. First, numerical simulations demonstrated that a spinning 2D soliton in such a model seems quite stable [12]. Next, direct simulations of

the spinning solitons in the same cubic-quintic model have revealed that the solitons are always subject to the azimuthal instability, but the instability may be fairly weak if the size of the soliton is essentially larger than the radius of its internal hole [13]. In the latter case, the spinning soliton may be a virtually stable object in an experiment. In fact, the same pertains to the 2D solitons: the stability reported in [12] is, actually, a weak instability, masked by relatively short simulation runs.

Thus, the challenge is to seek a realistic nonlinear optical models which may generate truly stable spinning solitons. In this paper, we demonstrate that this is possible both in the usual optical fibre, provided that it admits the propagation of the lowest-order helical mode, and in a bulk medium combining  $\chi^{(2)}$  and self-defocusing  $\chi^{(3)}$  (cubic) nonlinearities.

## 2. Helical solitons in optical fibres

### 2.1 Formulation of the problem

A commonly adopted approach to the description of nonlinear light propagation in optical fibres is based on the separation of the transverse modal structure, that may be described in the linear approximation, and slow longitudinal and temporal evolution of the signal's envelope, which is essentially affected by the temporal dispersion and Kerr nonlinearity. This type of analysis leads to the derivation of the nonlinear Schrödinger (NLS) equation for the envelope [1,2].

Usually, both experimental and theoretical studies of the soliton propagation are confined to the case when parameters of the fibre admit a single (fundamental) transverse mode, because in a multimode fibre an initial pulse excites different modes in an uncontrollable fashion. However, using well-known data for fibres of the simplest step-index type [14], it is easy to find that a situation with exactly two modes takes place when the standard *waveguide parameter*

$$V \equiv k\rho \sqrt{n_{\text{co}}^2 - n_{\text{cl}}^2}, \quad (1)$$

where  $k$ ,  $\rho$  and  $n_{\text{co,cl}}$  are, respectively, the carrier wave's propagation constant, core radius, and the refractive index in the core and cladding, takes values

$$2.405 < V < 3.832. \quad (2)$$

For instance, in the case of the standard carrier wavelength ( $\lambda = 1.54 \mu\text{m}$ ) admitting soliton propagation in optical fibres, and taking the usual value  $n_{\text{co}} - n_{\text{cl}} = 0.01$ , the interval (2) implies  $3 \mu\text{m} < \rho < 4.75 \mu\text{m}$ , i.e., quite realistic values of the core's radius.

Inside the interval (2), the fibre carries a fundamental mode (FM) and the first helical mode (HM). The transverse structure of the latter is described by the expressions  $J_1(Ur) \exp(\pm i\theta)$  in the core and  $K_1(Wr) \exp(\pm i\theta)$  in the cladding, where  $J_1$  and  $K_1$  are the standard cylindrical functions,  $U$  and  $W$  are the associate waveguide parameters defined in the usual way [14], and  $(r, \theta)$  are the polar coordinates in the fibre's cross section. In this case, one is actually dealing with a set of three coexisting modes, as there are two degenerate HMs with the helicities  $S = \pm 1$ . Note also that, because the physical fields are proportional to the real part of the complex expressions, the presence of the multiplier

$\exp(\pm i\theta)$  means that HM solitons are indeed *spinning* in the course of propagation along the fibre.

As neither higher-order radial (nonhelical) modes, nor any HM with a helicity  $> 1$  exists in the interval (2), the two-mode situation is controllable: a light pulse with zero helicity can excite solely the FM, while excitation of the HM is possible by a pulse that carries the necessary helicity. A light beam can be lent helicity, passing it through a specially designed phase mask, which is quite feasible in a real experiment, see, e.g., the above-mentioned work [9], where this technique was employed to create a spatial cylindrical soliton with the intrinsic vorticity. Due to their distinct topological nature, FMs and HMs do not mix linearly, provided that the fibre remains circular. It is indeed easy to fabricate a long silica fibre whose deviation from circularity is negligible. Bending of the fibre will induce no linear mixing either, providing that the bending radius is much larger than the wavelength. In this paper, however, we do not discuss exact limitations on the deviation of the fibre from circularity and similar details. Instead, we focus on principal issues, such as collisions between solitons carried by FMs and HMs.

It is necessary to distinguish between the fundamental and helical solitons at the receiver end of the fibre. In an experiment with a single or a few copropagating carrier frequencies, this is quite simple, as the fundamental and helical modes have an appreciable difference in their propagation constants (see below), thus the two types of the solitons can be distinguished by means of a simple wavelength filter. Besides that, there is a possibility to create a ‘helicity filter’, which would also work in the case of a multi-channel WDM system. Indeed, if it is known that two species of solitons in the fibre have the helicities  $S = 0$  and  $S = +1$ , at the receiver end, the incoming signal can be passed through a phase mask that adds extra helicity  $\Delta S = -2$ . Then, the arriving FM and HM solitons will change their helicities to  $-2$  and  $-1$ , respectively, so that only the latter will survive, as in the selected parametric region the modes with  $S = \pm 2$  do not propagate in the fibre. On the other hand, passing the incoming signal through the phase mask which adds  $\Delta S = +1$  will transform the former  $S = 0$  soliton into a propagating  $S = +1$  pulse, while the former  $S = +1$  soliton will have  $S = +2$ , hence it will not be able to propagate.

Thus, by launching solitons independently in each of the two modes, one can implement a two-channel system inside the core. Note that the standard elements of fibre communication systems, such as amplifiers and guiding filters [2], will act in essentially the same way on the solitons in both modes (although the gain coefficients of an Er-doped fibre amplifier may differ for the two modes, depending on the density distribution of the doping atoms in the fibre’s transverse plane). Moreover, if one starts with a WDM multichannel system already implemented in the fibre, one can *double* the number of the channels by means of this two-mode scheme. It will be shown below that it is not really possible to triple the number of the channels, using two HMs with opposite helicities. The feasibility of such a ‘mode-division’ channel doubling may be quite important, as it has been demonstrated that doubling by means of the polarization-division multiplexing is incompatible with WDM [15]. Indeed, while the polarization of the soliton can be easily changed by various imperfections of the system, the mode’s helicity is expected to be robust, as it is a *topological invariant*. Note that we do not consider the polarization structure of the modes, assuming that either they belong to one polarization, or (more realistically for the applications) the polarization can be effectively averaged out. Thus, our helical mode has nothing in common with the circular polarization.

Due to the Kerr nonlinearity, the linearly orthogonal solitons borne by the two modes interact via the cross-phase modulation (XPM). The main effect considered in this part of the paper is collisions between the solitons. As is well known, the collisional crosstalk is the most fundamental problem in soliton-based multichannel communication systems, see, e.g., refs [16–18].

It should be stressed that, while the application of the proposed mode-division doubling to WDM soliton communication systems is not straightforward, as there remain some technical problems, experimental observation of narrow *subpicosecond* helical (spinning) solitons and collisions between themselves and with fundamental solitons in relatively short optical fibres is a problem of fundamental physical interest in itself. A combination of the above-mentioned helicity-generating phase masks with the well-developed experimental technique admitting, e.g., direct observation of the polarization structure of subpicosecond solitons in short fibres [19] should make the observation of the helical solitons and their collisions quite feasible.

It is also noteworthy that the helical soliton, whose local intensity vanishes at the central point of the fibre's cross section, may be a natural object to exist in *hollow* nonlinear optical fibres, which have recently attracted a lot of attention (and where, incidentally, very narrow solitary pulses are quite possible), see, e.g. [20] and references therein.

## 2.2 The model

A normalized system of coupled nonlinear Schrödinger (NLS) equations for the interacting modes can be derived by means of a standard asymptotic procedure [1],

$$i(u_0)_z + ic_0(u_0)_\tau + k_0 u_0 - \frac{1}{2}\beta_0(u_0)_{\tau\tau} + (|u_0|^2 + 2\gamma_0|u_+|^2 + 2\gamma_0|u_-|^2)u_0 = 0, \quad (3)$$

$$i(u_+)_z + ic_1(u_+)_\tau + k_1 u_+ - \frac{1}{2}\beta_1(u_+)_{\tau\tau} + (|u_+|^2 + 2|u_-|^2 + 2\gamma_1|u_0|^2)u_+ = 0, \quad (4)$$

$$i(u_-)_z + ic_1(u_-)_\tau + k_1 u_- - \frac{1}{2}\beta_1(u_-)_{\tau\tau} + (|u_-|^2 + 2|u_+|^2 + 2\gamma_1|u_0|^2)u_- = 0 \quad (5)$$

(In the case of extremely narrow solitons, well-known higher-order terms [1,2] should be added to the system.) We here consider the most general case, when two HMs with the helicities  $\pm 1$ , represented by the envelopes  $u_\pm$ , interact with the zero-helicity FM  $u_0$ ;  $\beta_0$  and  $\beta_1$  are the corresponding mode-dependent dispersion coefficients (see below),  $c_{0,1}$  and  $k_{0,1}$  are the group-velocity and propagation-constant shifts of the two modes (these characteristics are also mode-dependent [14]), and the effective XPM coefficient  $\gamma_0$  and  $\gamma_1$  are given by the properly normalized overlapping integrals between FM and HM. Using known expressions for the transverse modal functions of the step-index fibre [14], we have calculated them numerically. In figure 1a, we display  $\gamma_0$  and  $\gamma_1$  vs. the waveguide parameter (1).

Note that eqs (3)–(5) do not contain four-wave mixing (FWM) terms. Some of them might originate from the terms  $\sim u_0^2 (u_\pm^*)^2$  and its complex conjugate in the model's Hamiltonian density. However, the full expressions to be inserted into the Hamiltonian are multiplied by the modal angular dependencies  $\exp(\mp 2i\theta)$ , hence they will give zero upon angular integration. Another possible source of FWM terms in eqs (3)–(5) could be the

term  $\sim u_0^2 u_+^* u_-^*$  and its complex conjugate in the Hamiltonian density. In these expressions, the angular dependence cancels out, hence the angular integration will not nullify them. However, the corresponding terms in eqs (3)–(5) will be rapidly oscillating in  $z$  because of the difference between the propagation constants  $k_0$  and  $k_1$ . A straightforward consideration yields an estimate for the relative wavenumber mismatch between FM and HM in the region of interest,  $|k_1 - k_0|/k \approx 0.4 (n_{co} - n_{cl})$ . Taking the same estimate for the refractive index difference as above,  $n_{co} - n_{cl} \approx 0.01$ , we conclude that  $|k_1 - k_0|/k \sim 0.005$ , which corresponds to the beat length  $\sim 200$  wavelengths. As it is small in comparison with any propagation distance relevant to solitons, all the FWM terms may be neglected.

As for the dispersion coefficients in eqs (1)–(3), their components accounted for by the waveguide geometry can also be calculated for the two modes on the basis of the data available from linear-propagation theory [14]. The result of the calculation is shown in figure 2b. It is noteworthy that the waveguide-geometry component of  $\beta_0$  changes its sign. One should, however, keep in mind that the full dispersion also contains a material (bulk) contribution, which may be essentially larger than that displayed in figure 1b.

Thus, the analysis of the interaction between solitons must admit *different* (but both negative, i.e., anomalous [1]) effective dispersions  $\beta_0$  and  $\beta_1$  in eqs (3)–(5). Together with the nonstandard values of the XPM coefficients  $\gamma_0$  and  $\gamma_1$ , these features constitute an essential mathematical difference of the present model from a usual three-channel WDM one (see, e.g., ref. [17]).

The fundamental and helical modes are also characterized by a difference in their group velocities, which plays a crucially important role in the analysis of soliton-soliton collisions. Continuing the above estimates of the physical parameters for the present case, we obtain

$$(\delta v_{gr})_{mode} / v_{gr} \sim 5 \cdot 10^{-6} \tag{6}$$

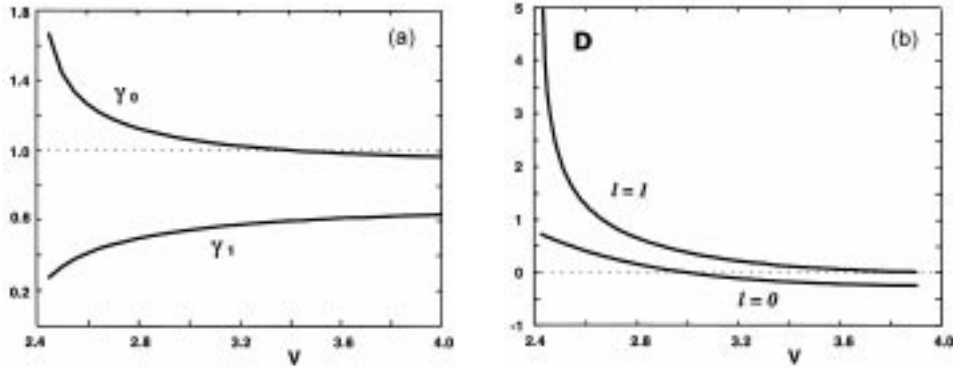


**Figure 1.** The normalized XPM coefficients (a) and the normalized waveguide dispersion coefficients (b), vs. the waveguide parameter  $V$  for the fundamental ( $S = 0$ ) and helical ( $S = 1$ ) modes in the standard step-index fibre. The full waveguide dispersion is  $(n_{cl} V \Delta / \lambda c) D$ , where  $c$  is the velocity of light, and  $\Delta \equiv (n_{co} - n_{cl}) / n_{co}$ . In plot (a), the dashed line shows the usual value ( $\equiv 1$ ) of the XPM coefficient.

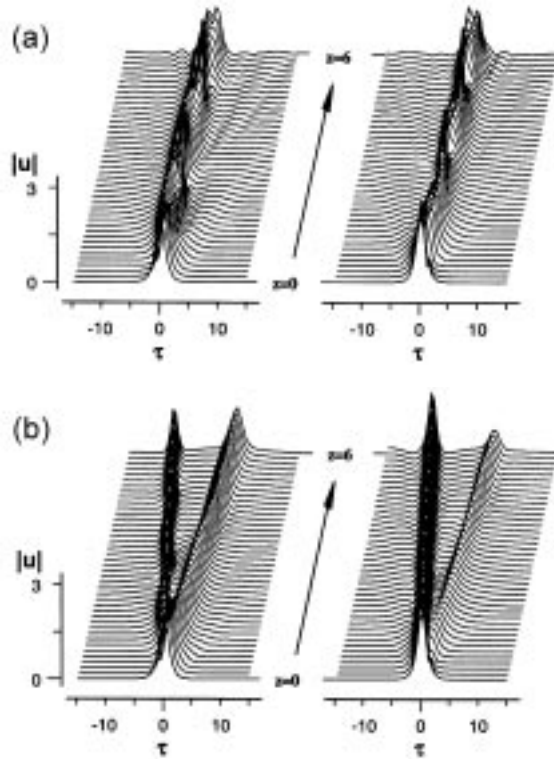


**Figure 2.** Collisions of initially overlapped solitons with amplitudes  $|u|_{\max} = |v|_{\max} = 2$  and the relative inverse group velocity  $c_1 - c_0 = 29$  (recall it must be a large parameter) simulated with eqs (1) and (2), in which  $\beta_0 = \beta_1 = -1$ : **(a)** the usual WDM system, with  $\gamma_0 = \gamma_1 = 1$ ; **(b)** the fundamental and helical solitons, with  $\gamma_0 = 0.98$  and  $\gamma_1 = 0.62$ . The simulations were carried out from  $z = 0$  up to a distance equal to six soliton periods, which is  $z = 6$ .

for the relative group-velocity difference between the modes. As concerns the possibility to use the mode-division doubling of the channels in the WDM system, it is relevant to mention that, in the WDM system implemented in a standard telecommunications fibre with dispersion  $\beta \sim -20 \text{ ps}^2/\text{km}$  at  $1.54 \mu\text{m}$ , the relative group-velocity mismatch between the adjacent channels is estimated to be

$$(\delta v_{\text{gr}})_{\text{WDM}}/v_{\text{gr}} \sim 10^{-2} \cdot (\delta\lambda/\lambda), \quad (7)$$

$\delta\lambda$  being the wavelength separation between the channels. The case of practical interest is  $\Delta\lambda \sim 1 \text{ nm}$ , hence we conclude that the relative group-velocity differences (6) and (7) are of the same order of magnitude. On the other hand, in the dispersion-shifted (DS) or dispersion-compensated (DC) fibres, the effective value of the dispersion is much smaller than the above-mentioned value  $-20 \text{ ps}^2/\text{km}$ , hence in these cases the inference is that the corresponding WDM relative difference is negligible compared to that between the fundamental and helical modes,

$$(\delta v_{\text{gr}})_{\text{WDM}}^{(\text{DS/DC})} / v_{\text{gr}} \ll (\delta v_{\text{gr}})_{\text{mode}} / v_{\text{gr}}. \quad (8)$$

For typical solitons used in telecommunications, with temporal width  $T \sim 10$  ps, the above estimate  $(\delta v_{\text{gr}})_{\text{mode}} / v_{\text{gr}} \sim 5 \cdot 10^{-6}$  implies that a collision between the FM and HM solitons takes place at a propagation distance  $z_{\text{coll}} \sim T (\delta v_{\text{gr}})_{\text{mode}} / v_{\text{gr}}^2 \sim 500$  m, which is much shorter than any soliton's length scale. This circumstance allows us to treat the XPM-mediated interaction as a small perturbation in the course of the fast passage of one soliton through the other, as it was done in other contexts in [17,18]. Note that in the laboratory experiments with subpicosecond solitons, the collision length may be  $\lesssim 50$  m, implying that the experimental study of the collisions should be quite possible.

On the other hand, there is no group-velocity difference between the two HMs  $u_{\pm}$ , hence the collision distance for the corresponding solitons may be very large, giving rise to a strong crosstalk between them. Moreover, the collision between two solitons with the helicities  $S = \pm 1$  may result in their annihilation or transformation into a pair of  $S = 0$  solitons, while, due to the conservation of the topological invariant, the collision between the solitons with  $S = 0$  and  $S = 1$  is expected to be much closer to an elastic one. In view of this, it makes sense to assume only the doubling of the number of channels by means of the 'mode-division multiplexing' (i.e., to use only one HM) in the context of the WDM systems, but not tripling, that might seem possible due to the existence of two HMs with  $S = \pm 1$ . Irrespective of that, a study of collisions between the solitons with  $S = +1$  and  $S = -1$  is a challenge for experiments with narrow solitons in optical fibres.

### 2.3 Analytical treatment of soliton collisions

Proceeding to the perturbative analysis of the collision between the solitons carried by FM and HM, we should take into consideration that, in view of the asymmetry between eqs (3) and (4), (5), the FM and HM solitons may have *different* widths,  $T_0$  and  $T_1$ . This circumstance makes it technically impossible to base the perturbative treatment of the collision on the exact unperturbed soliton waveforms of the sech type, as the corresponding overlap integrals will be intractable. The only possibility to develop an efficient perturbation theory is to use, as the zero-order approximation, the Gaussian *ansatz* for the unperturbed soliton solutions to the uncoupled equations (3) and (4),

$$u_l^{(0)}(z, \tau) = A_l \exp \left( iK_l z - \frac{(\tau - t_l)^2}{2T_l^2} \right), \quad \frac{dt_l}{dz} = c_l; \quad l = 0, 1, \quad (9)$$

where a relation between the amplitude and width of the soliton can be found by means of the variational approximation [21],

$$A_l^2 = \sqrt{2} |\beta_l| / T_l^2 \quad (10)$$

(the propagation constants  $K_l$  will not be needed here). In fact, the difference between the approximate soliton's shape given by eq. (9) and the exact sech shape is fairly small, see, e.g., figure 5 in [21].

A soliton moving in the given reference frame is obtained from eq. (9) as its Galilean transform,

$$u_l(z, \tau) = u_l^{(0)}(z, \tau - t_l(z)) \exp(-i\omega_l \tau + iqz), \quad (11)$$

where  $\omega_l$  is an arbitrary transform-generating frequency shift, the propagation-constant shift  $q$  is not essential, and (cf. eq. (9))

$$\frac{dt_l}{dz} = c_l - |\beta_l| \omega_l. \quad (12)$$

If the XPM term in eqs (1)–(3) is, effectively, a small perturbation (in the case of a fast collision, see above), the collision between the solitons may be described as that between two quasiparticles interacting through an effective potential. Following the lines of the analysis developed for similar problems earlier [17,18], it is straightforward to derive the following perturbation-induced evolution equations for the solitons' frequency shifts:

$$\frac{d\omega_l}{dz} + \frac{4|\beta_l|\gamma_l}{T_{1-l}\sqrt{T_0^2 + T_1^2}} \cdot \frac{d}{dt_l} \exp\left[-\frac{(t_1 - t_0)^2}{2(T_0^2 + T_1^2)}\right] = 0, \quad (13)$$

where eq. (10) was used to eliminate the amplitudes in favour of the widths  $T_l$  (recall that  $\gamma_l$  are the relative XPM coupling constants in eqs (3)–(5)). Combining eq. (13) with eq. (12) and assuming, in the first approximation,  $T_l = \text{constant}$ , furnishes a closed dynamical system governing the evolution of the temporal positions  $t_l$  of the two solitons.

To further apply the perturbation theory to eq. (13), we recall that, according to the estimates obtained above, the difference of the inverse group velocities,  $c \equiv c_1 - c_0$ , is, effectively, a large parameter. Hence, in the lowest-order approximation, one may set  $t_1 - t_0 \approx cz$  in the argument of the exponential in eq. (13), thus strongly simplifying the equation:

$$\frac{d\omega_l}{dz} = \frac{4(-1)^l |\beta_l| \gamma_l}{c T_{1-l} \sqrt{T_0^2 + T_1^2}} \cdot \frac{d}{dz} \exp\left[-\frac{(cz)^2}{2(T_0^2 + T_1^2)}\right]. \quad (14)$$

To proceed, it is necessary to specify the type of collision to be considered. One should distinguish between 'complete' and 'incomplete' collisions [18]. In the former case, the solitons are, originally, far separated; in the course of the interaction, the faster soliton catches up with the slower one and passes it. In the first approximation, the complete interaction does not give rise to a net frequency shift (a change of the frequency would be tantamount to a change of the soliton's velocity, according to eq. (12)), as the integration of the right-hand side of eq. (14) from  $z = -\infty$  to  $z = +\infty$  yields zero. However, finding a nonzero *instantaneous* frequency shift from eq. (14), inserting it into eq. (12), and integrating the latter equation yield a nonzero collision-induced *position* shift  $\delta t_l$  of the soliton's centre, which is the main effect of the complete collision. A final result can be conveniently written as a relative position shift, normalized to the soliton's temporal width:

$$\frac{\delta t_l}{T_l} = (-1)^{l-1} \cdot 4\sqrt{2\pi} \frac{\beta_0 \beta_1}{c^2 T_0 T_1} \gamma_l. \quad (15)$$

An 'incomplete' collision takes place if the solitons are essentially overlapped at the initial point,  $z = 0$ . This kind of collision is more significant, as it gives rise to a nonzero net frequency shift  $\delta\omega_l$  (hence, to a velocity shift too). The most important (dangerous)

case is when the centres of the colliding solitons exactly coincide at  $z = 0$ . In this case,  $\delta\omega_l$  is found by straightforward integration of eq. (14) from  $z = 0$  to  $z = +\infty$ . The result can be presented in a more natural form, multiplying the net frequency shift by the soliton's temporal width (i.e., normalizing the frequency shift to the soliton's spectral width):

$$T_l \delta\omega_l = 4(-1)^{l-1} \frac{|\beta_l| T_l}{c T_{1-l} \sqrt{T_0^2 + T_l^2}} \gamma_l. \quad (16)$$

The only difference of eqs (15) and (16) from similar results for the usual WDM system are the specific XPM coefficients  $\gamma_l$ , which are  $\equiv 1$  in the usual case. The most promising range for the applications is around  $V = 3.6$  (figure 1a), which gives

$$\gamma_0 \approx 0.98, \gamma_1 \approx 0.62. \quad (17)$$

This implies that the crosstalk between the FM and HM solitons is attenuated by the factor 0.62 for the HM soliton, as compared to the usual WDM system, while for the FM soliton the crosstalk strength is not different from that in the usual system (taking, instead, the values around  $V = 2.4$  (figure 1a), we will get small  $\gamma_1 \approx 0.25$ , but large  $\gamma_0 \approx 1.66$ ).

Thus, if the set of the HM and DM modes is used to double the number of channels in the WDM system, we conclude that the crosstalk for the HM solitons due to their collisions with the FM ones in any channel is attenuated, against the usual crosstalk strength, by the above-mentioned factor  $\approx 0.62$ .

Note that the conclusion concerning the comparison with the WDM crosstalk pertains to the case when the WDM system is realised in the standard telecommunications fibre: as it was concluded above, in this case, the group-velocity difference between the fundamental and helical modes is of the same order of magnitude as the group-velocity mismatch between adjacent WDM channels, see eqs (6) and (7). Contrary to this, in the dispersion-shifted or dispersion-compensated fibre link, the group-velocity difference between the FM and HM channels is much larger than that between the WDM ones, hence the FM-HM crosstalk is much weaker than between the WDM channels, according to eqs (15) and (16).

#### 2.4 Numerical simulations of the collision

Direct simulations of the soliton collisions within the framework of eqs (3) and (4) for the two modes demonstrate that, although the above-mentioned frequency-shift-attenuation factor 0.62 is not really small, sometimes it may be important. In figure 2a, we display an example of a disastrous *incomplete* collision in the usual WDM system, which leads to a merger of the solitons into a *breather* (the simulations of the complete collision at the same values of the parameters shows that it is fairly mild, producing only small position shifts of the solitons). Replacing the usual XPM coefficients  $\gamma \equiv 1$  by those for the FM-HM collision, given by eq. (17), we find that the same solitons *survive* the incomplete collision (figure 2b).

### 3. Vortex-ring solitons in a bulk medium

Since the pioneering experimental results reported in [22] (see also an independent theoretical prediction in [23]), *optical* vortices have been of great interest. Formally, conventional

vortices require an infinite nonzero background, which in practice necessitates a host beam with a large transverse beam to observe vortices [24].

A different possibility is to consider bright spatial solitons, i.e., *ring* solitons in the form of bright self-guided beams with an internal vorticity. As it was mentioned above, recent theoretical [8] and experimental [9] studies have shown that ring solitons are strongly unstable against azimuthal perturbations in materials with purely quadratic or saturable nonlinearities (in which zero-vorticity bright solitons are well known to be stable).

Materials with a mixed nonlinear response may prove to be more promising. Using a model describing optical media with a cubic-quintic nonlinear response, rings that were apparently stable against both small perturbations and collisions between two rings, were reported in the above-mentioned paper [12]. However, longer simulations demonstrate that these ring vortices (in both (2 + 1)- and (3 + 1)-dimensional cases) are also subject to instability against azimuthal perturbations [13]. Thus, a challenging fundamental question is whether truly stable ring solitons can exist in some model with a realistic nonlinearity. In this part of the paper, we produce a model which indeed supports stable ring solitons in optical media with both  $\chi^{(2)}$  and  $\chi^{(3)}$  nonlinearities. The stability of rings in these media will be demonstrated by direct simulations (including collisions), and also by full-scale linear-stability analysis. The corresponding derivation procedure closely follows that developed in [25], yielding a normalized system of coupled equations for the fundamental- and second-harmonic (FH and SH) fields  $u$  and  $w$ ,

$$\begin{aligned} i\frac{\partial u}{\partial z} + \nabla^2 u - \beta u + u^* w + \chi(|u|^2/4 + 2|w|^2)u &= 0, \\ 2i\frac{\partial w}{\partial z} + \nabla^2 w - \alpha w + \frac{u^2}{2} + \chi(4|w|^2 + 2|u|^2)w &= 0, \end{aligned} \quad (18)$$

where  $\nabla^2 \equiv \partial^2/\partial x^2 + \partial^2/\partial y^2$  is the transverse diffraction operator,  $\alpha \equiv (2\Delta + 4\beta)$ ,  $\beta$  is a nonlinear shift of the fundamental-harmonic's propagation constant,  $\Delta$  is the normalized wave-vector mismatch, and  $\chi = \pm 1$  is the parameter to distinguish between self-focusing or self-defocusing Kerr nonlinearity. In this work, we set  $\chi = -1$ , which corresponds to the self-defocusing case. Stationary localised solutions with zero and non-zero vorticity ('spin' or topological charge)  $n$  have the form  $u = U(r) \exp(in\phi)$  and  $w = W(r) \exp(2in\phi)$ , where  $r$  and  $\phi$  are the polar coordinates in the transverse plane. Below, we deal with rings for which  $n = \pm 1$ . Real radial profiles  $U(r)$  and  $W(r)$  are to be found as localised solutions of the system

$$\begin{aligned} \frac{d^2 U}{dr^2} + \frac{1}{r} \frac{dU}{dr} - \frac{n^2 U}{r^2} - \beta U + UW - (U^2/4 + 2W^2)U &= 0, \\ \frac{d^2 W}{dr^2} + \frac{1}{r} \frac{dW}{dr} - \frac{4n^2 W}{r^2} - \alpha W + \frac{U^2}{2} - (4W^2 + 2U^2)W &= 0, \end{aligned} \quad (19)$$

We solved eqs (19) by means of the standard relaxation technique, finding domains of existence of different localised solutions with zero and non-zero values of the vorticity. Typical examples of the localised radial profiles are shown in figure 3. When the soliton parameter  $\beta$  is small (a low-power regime), ring solitons are rather narrow. The beam's amplitude at first increases with  $\beta$ , but for larger values of  $\beta$  it saturates, while the ring width broadens

because of the self-defocusing influence of the  $\chi^{(3)}$  term. The ring soliton family bifurcates from conventional vortex solitons (with non-zero asymptotics) at some  $\beta_{cr}(\Delta)$  which is the upper boundary of the diagonally hashed region in figures 4 and 8. The change of the ring shape with changing  $\beta$  is qualitatively similar to that in the cubic-quintic model, where the competition of self-focusing and defocusing takes place too [12,13]. Such similarities are not surprising because in the *cascading limit* of large  $\Delta$  the SH component can be eliminated as  $w \approx u^2/(4\Delta)$ , and the remaining equation for the FH field reduces to the cubic-quintic model. Results for the existence and modulational stability of various types of solitons of eqs (18) are summarized in the form of a diagram in the parametric plane  $(\Delta, \beta)$ , (figure 4). Its noteworthy feature is coexistence of vortex, ring-vortex, ring, and conventional (zero spin) bright solitons. Note that ring-vortex solitons in eqs (18) with  $\chi = -1$  and  $\beta < 0$  were first found in a recent work [26] for a rescaled version of eqs (18). At  $\beta < 0$ , these pairs bifurcate from the single-component (SH-only) finite-background vortices along the *D*-curve in figure 4. Our analysis demonstrated that all these ring-vortex soliton pairs are unstable. At  $\beta > 0$ , the ring-vortex pairs are a continuation of rings: these two types of solutions merge when the SH background vanishes. It follows immediately from the second equation in the system (19), that this happens at  $\Delta = -2\beta$ , on the line *A* in figure 4. On the other side of the existence domain, the ring-vortex pairs bifurcate from modulationally stable two-component finite-background vortices. This bifurcation curve does not always coincide with the existence boundary of the finite-background vortices (curve *C*). At  $\beta < 0$ , it is given by the line  $\Delta = -0.5$ . Below, we concentrate on the central subject of our analysis – fundamental ( $n = \pm 1$ ) rings and their stability. In fact, the stability of the rings is a very complex issue. Here, we address the stability problem first by simulating the propagation of azimuthally perturbed ring solitons and their collisions. The split-step Fourier (beam propagation) method was used to solve eqs (18). A general conclusion strongly suggested by results of the simulations is as follows: rings which are close enough to the upper boundary of the existence domain (i.e., broad flat-top rings) are stable, whereas more localised ones are unstable against azimuthal instabilities. This

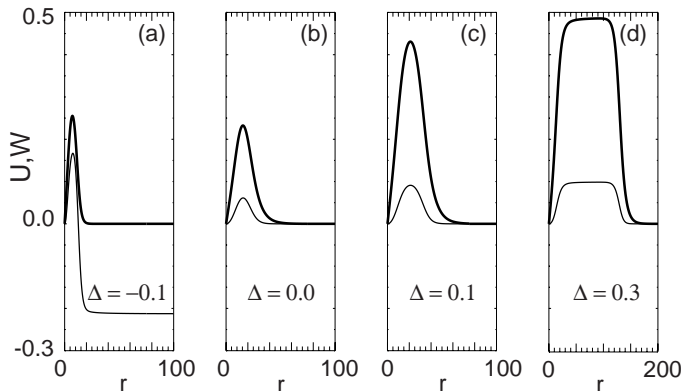


**Figure 3.** Examples of an ring-vortex soliton pair (a) and rings (b, c, d) for  $\beta = 0.02$  and different values of  $\Delta$ . Thick and thin curves stand for the first- and second-harmonic radial functions  $U(r)$  and  $V(r)$ .

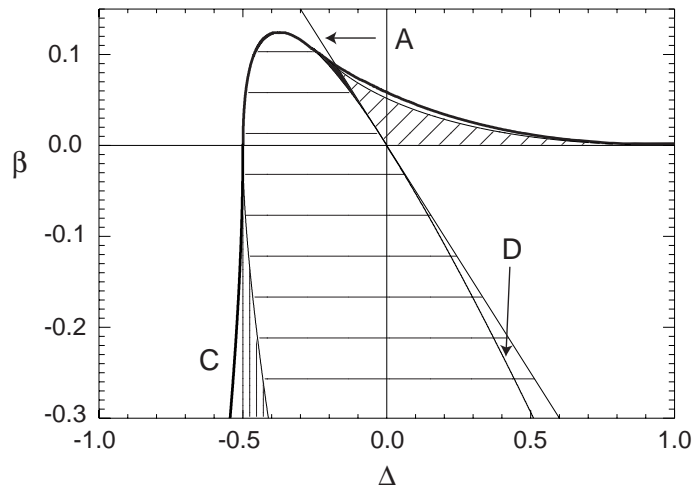


**Figure 4.** Regions of existence and modulational stability (for solitons with non-zero asymptotics) of various types of solitons in the  $(\Delta, \beta)$  plane. Conventional vortices exist everywhere below the thick curve C, which also indicates the boundary of the modulational stability for the vortex background plane waves. The meaning of the lines A and D is explained in the text. The existence domain for rings and zero spin bright solitons is diagonally hashed. A domain of the existence of modulationally unstable ring-vortex solitons is horizontally hashed. For  $\beta < 0$ , the existence domain for modulationally stable ring-vortices is vertically hashed. At  $\beta > 0$ , modulationally stable ring-vortices were found in a small black domain.

conclusion is consistent with recent results obtained for the cubic-quintic model, where it was clearly shown that making the ring broader strongly, but *not* completely, suppressed its azimuthal instability [13]. Our simulations show that (relatively) narrow unstable rings with the spin  $n = \pm 1$  break up into two filaments, which is a generic outcome of the development of the azimuthal instability in the saturable and cubic-quintic models as well [8,10,13]. Broad ring solitons may survive their collisions (see figure 5). Direct simulations of the stability may be sufficient to predict experimental observation of stable rings, but it is not sufficient to resolve the principle issue of the stability: as it was argued in [13], an instability may be missed if the simulations are not long enough, which was the case in [12]. Thus, it is necessary to perform a direct linear stability analysis of the rings in the present model. To this end, consider infinitesimal complex perturbations  $\varepsilon(z, r, \theta)$  added to the stationary solutions of eqs (18),

$$\begin{aligned} u &= [U(r) + \varepsilon_1(z, r, \theta)]e^{in\theta}, \\ w &= [W(r) + \varepsilon_2(z, r, \theta)]e^{2in\theta} \end{aligned} \tag{20}$$

where  $n$  is the value of topological charge as before,  $U$  and  $W$  being stationary solutions. The perturbation  $\varepsilon_m(z, r, \theta)$  is taken as

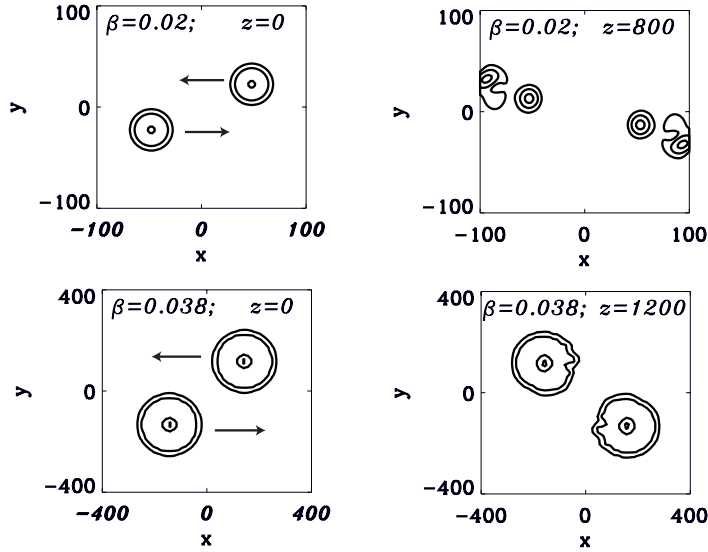


**Figure 5.** Collisions between unstable (upper) and stable (lower) ring solitons of eqs (18) at  $\Delta = 0.1$ . Note that the usually unstable ring splits into two zero-vorticity bright solitons, and rings which survive the collision are rather broad.

$$\epsilon_m = \sum_J \left[ \xi_{Jm}^+(r) e^{i(\lambda z + J\theta)} + \xi_{Jm}^-(r) e^{-i(\lambda^* z + J\theta)} \right], \quad (21)$$

where  $J = 0, \pm 1, \pm 2, \dots$  is the extra vorticity of the perturbation term. Substituting the ansatz (20) into eqs (18) and linearizing, we get the following non-self-adjoint eigenvalue problem,

$$\lambda \vec{\xi}_J = \begin{bmatrix} A_+ & B & C & D \\ -B & -A_- & -D & -C \\ C/2 & D/2 & E_+/2 & F/2 \\ -D/2 & -C/2 & -F/2 & -E_-/2 \end{bmatrix} \vec{\xi}_J, \quad (22)$$

where  $\vec{\xi}_J \equiv (\xi_{J1}^+, \xi_{J1}^-, \xi_{J2}^+, \xi_{J2}^-)$ ,  $A_{\pm} = \hat{L}_{J1}^{\pm} + \chi(U^2/2 + 2W^2)$ ,  $B = W + \chi U^2/4$ ,  $C = U + 2\chi UW$ ,  $D = 2\chi UW$ ,  $E_{\pm} = \hat{L}_{J2}^{\pm} + 2\chi(4W^2 + U^2)$ ,  $F = 4\chi W^2$ , and we define operators

$$\hat{L}_{J1}^{\pm} \equiv \frac{\partial^2}{\partial r^2} + \frac{1}{r} \frac{\partial}{\partial r} - \frac{1}{r^2} (n \pm J)^2 - \beta, \quad (23)$$

$$\hat{L}_{J2}^{\pm} \equiv \frac{\partial^2}{\partial r^2} + \frac{1}{r} \frac{\partial}{\partial r} - \frac{1}{r^2} (2n \pm J)^2 - (4\beta + 2\Delta).$$

Unstable eigenmodes have eigenvalues with non-zero imaginary part. (As the present model is Hamiltonian eigenvalues appear in complex conjugate quadruplets or pairs.) Real

eigenvalues which lie in the range  $(\Gamma, \infty)$  or  $(-\Gamma, -\infty)$ , where  $\Gamma \equiv \min(\beta, 4\beta + 2\Delta)$ , belong to the continuous spectrum.

To analyse the eigenvalue problem (22), the differential operators were replaced by their fifth-order finite-difference approximations and the resulting algebraic eigenvalue problem was solved numerically. Most often, 200–400 grid points were used in the analysis, but up to 1200 points were used in parameter regions where a change of the stability occurs. To verify the precision of our numerical method, a technique based on the relaxation method for solving two-point boundary value problems was used too. Although limited to finding only internal modes (eigenmodes with  $\lambda$  purely real), the relaxation method admits a high degree of control over precision without much of the computational overhead of other numerical methods. Note that this method has been recently used to a great effect in finding a small stability window for higher-order spatial solitons in the parametric-third-harmonic generation model, which would have otherwise been thought to be unstable [27]. The comparison between the spectral and relaxation methods has shown that the former one has a good precision for the number of grid points used. Results of the linear stability analysis are displayed in figures 6 and 8. The findings are in agreement with results of direct simulations of the propagation presented above: thin rings are unstable and broad rings are stable. Azimuthal perturbations with  $J = 0, \dots, \pm 5$  were analysed, and it has been found that dominant instability terms have  $J = \pm 2$ , eventually leading to the ring's breakup into two filaments. The eigenvalues associated with the  $J = \pm 2, \pm 3$  instability are complex. However, in all the cases analysed a *stability window* was found when  $\beta$  was approaching the upper existence boundary of ring solitons. For fundamental rings with the vorticity  $n = \pm 1$ , the stability window occupies up to  $\approx 8\%$  of the total existence domain  $[0, \beta_{\text{cr}}(\Delta)]$  of the ring solitons. In addition to fundamental rings, those with vorticity  $n = \pm 2$ , were also found to be stable albeit for a much smaller range of propagation constant  $\beta$

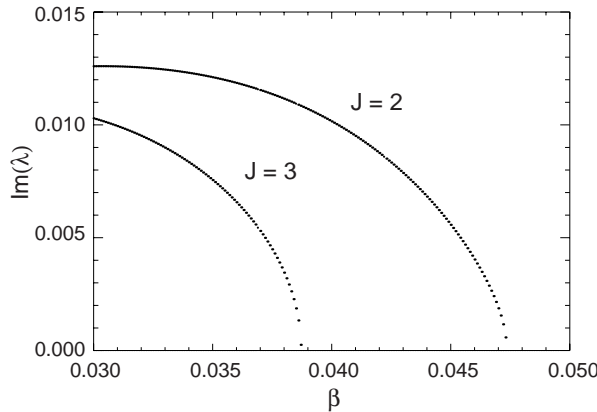


**Figure 6.** Unstable eigenvalues for  $\Delta = 0$ . Perturbation terms in eq. (4) with  $J = \pm 2$  account for a dominant instability, which is however no longer present for  $\beta \geq 0.0475$ ; the rings ( $n = \pm 1$ ) exist up to  $\beta \approx 0.0518$ . Perturbations with  $J = (\pm 1, \pm 4, \pm 5)$  have  $\text{Im } \lambda = 0$  within the numerical accuracy of our method, therefore they are not presented in this figure. Note, that both  $J = \pm 2$  and  $J = \pm 3$  related instabilities have complex eigenvalues (only  $\text{Im } \lambda$  parts are shown).

( $\approx 5\%$  of existence domain, see figure 7). Ring solitons with parameters belonging to the stability window propagate in the direct simulations without any visible perturbation growth indefinitely, surviving both azimuthal perturbations and collisions with other solitons. These are the first examples, in the authors' knowledge, of stable spinning solitons.

In several 1D models, solitons with non-fundamental profiles (multi-humped) have been found to be stable, or at least weakly unstable [28]. Recently, such solitons have been observed in experiments [29]. In some sense, ring solitons are analogous to double-humped solitons, while stable zero-spin one-hump bright solitons analysed in [30] represent a

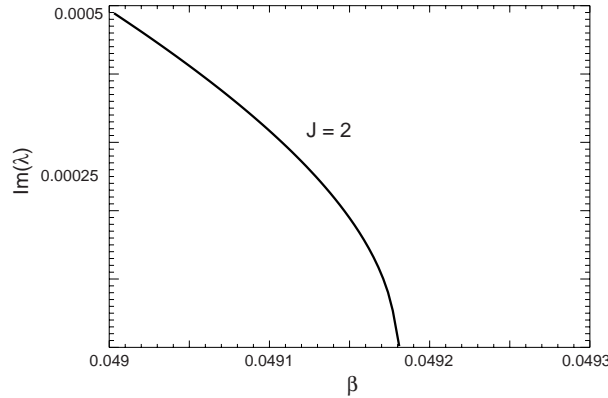


**Figure 7.** Same as figure 6 except only the eigenvalues associated with  $n = \pm 2$  rings and perturbation  $J = \pm 2$  (which is maximal). Stable rings with  $n = \pm 2$  exist for  $\beta \geq 0.04918$ .

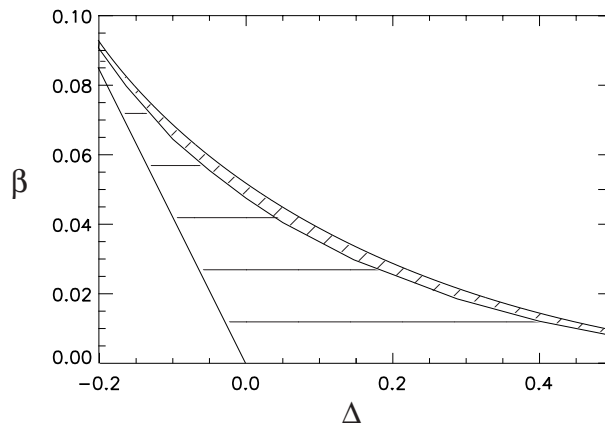


**Figure 8.** Region of existence and stability of fundamental ( $n = \pm 1$ ) rings of eqs (18). Region of stable rings is diagonally hashed while region of unstable rings is horizontally hashed.

fundamental soliton family of our model. Thus, the coexistence of stable solitons with the zero and nonzero topological charges resembles the above-mentioned cases of the coexistence between stable single- and double-humped solitons, reported in some of the papers [28]. However, a principal difference is that the zero- and nonzero-spin stable bright (2+1)D solitons coexist while belonging to *different topological classes*. Finally, it is necessary to address a possibility of experimental realization of optical media for observation of stable rings. Although no conventional nonlinear material with strong  $\chi^{(2)}$  nonlinearity directly satisfies our requirement to have a negative Kerr coefficient both for the FH and the SH frequencies, there are, at least, two schemes to effectively achieve this condition: (i) by building a layered medium in which some layers provide for the  $\chi^{(2)}$  nonlinearity, and others for the self-defocusing Kerr nonlinearity, or (ii) by engineering special nonlinear  $\chi^{(2)}$  gratings [31]. In the latter case, an average induced cubic nonlinearity can be provided for by a modulated quasi-phase-matching grating, that will be equal in strength to the intrinsic quadratic nonlinearity. Thus, media with the competing nonlinearities that may support stable vortex rings are within the reach of the modern-day experiment.

### Acknowledgements

Boris A Malomed acknowledges support from the Binational (US-Israel) Science Foundation and from the School of Electrical Engineering at the University of New South Wales (Sydney). Isaac Towers, Alexander V Buryak and Rowland A Sammut acknowledge support from the Australian Research Council.

The authors appreciate valuable discussions with P Di Trapani, F Lederer, D Mihalache, D V Skryabin and F Wise.

### References

- [1] G P Agrawal, *Nonlinear fiber optics* (Academic Press, San Diego, 1995)
- [2] A Hasegawa and Y Kodama, *Solitons in optical communications* (Oxford University Press, Oxford, 1995)
- [3] Y Silberberg, *Opt. Lett.* **15**, 1282 (1990)
- [4] L Bergé, *Phys. Rep.* **303**, 259 (1998)
- [5] A A Kanashov and A M Rubenchik, *Physica* **D4**, 122 (1981)
- [6] B A Malomed, P Drummond, H He, A Berntson, D Anderson and M Lisak, *Phys. Rev.* **E56**, 4725 (1997)  
D V Skryabin and W J Firth, *Opt. Commun.* **148**, 79 (1998)  
D Mihalache, D Mazilu, B A Malomed and L Torner, *Opt. Commun.* **152**, 365 (1998); **169**, 341 (1999)  
D Mihalache, D Mazilu, J Dörring and L Torner, *Opt. Commun.* **159**, 129 (1999)
- [7] X Liu, L J Qian and F W Wise, *Phys. Rev. Lett.* **82**, 4631 (1999)  
X Liu, K Beckwitt and F Wise, *Phys. Rev.* **E61**, R4722 (2000)
- [8] W J Firth and D V Skryabin, *Phys. Rev. Lett.* **79**, 2450 (1997)  
L Torner and D V Petrov, *Electron. Lett.* **33**, 608 (1997)  
D V Petrov and L Torner, *Quant. Electron.* **29**, 1037 (1997)
- [9] D V Petrov, L Torner, J Martorell, R Vilaseca, J P Torres and C Cojocar, *Opt. Lett.* **23**, 1444 (1998)

- [10] D Mihalache, D Mazilu, L-C Crasovan, B A Malomed and F Lederer, *Phys. Rev.* **E62**, R1505 (2000)
- [11] B L Lawrence, M Cha, J U Kang, W Torruellas, G Stegeman, G Baker, J Meth and S Etemad, *Electron. Lett.* **30**, 447 (1994)  
E W Wright, W Torruellas and G Stegeman, *Opt. Lett.* **20**, 2481 (1995)
- [12] M Quiroga-Teixeiro and H Michinel, *J. Opt. Soc. Am.* **B14**, 2004 (1997)
- [13] D Michalache, D Mazilu, L-C Crasovan, B A Malomed and F Lederer, *Phys. Rev.* **E61**, 7142 (2000)
- [14] A W Snyder and J D Love, *Optical waveguide theory* (Chapman and Hall, London, 1991)
- [15] J P Silmon-Clyde and J N Elgin, *Opt. Lett.* **23**, 180 (1998)
- [16] S Kumar, Y Kodama and A Hasegawa, *Electron. Lett.* **33**, 459 (1997)  
A N Niculae, W Forsyia, A J Gloag, J H B Nijhof and N J Doran, *Opt. Lett.* **23**, 1354 (1998)  
P V Mamyshev and L F Mollenauer, *Opt. Lett.* **24**, 448 (1999)
- [17] M J Ablowitz, G Biondini, S Chakravarty and R L Horne, *Opt. Comm.* **150**, 305 (1998)
- [18] D J Kaup, B A Malomed and J Yang, *Opt. Lett.* **23**, 1600 (1998)
- [19] Y Barad and Y Silberberg, *Phys. Rev. Lett.* **78**, 3290 (1997)
- [20] Y Tamaki, K Midorikawa and M Obara, *Appl. Phys.* **B67**, 59 (1998)  
Y Tamaki, Y Nagata, M Obara and K Midorikawa, *Phys. Rev.* **A59**, 4041 (1999)  
Z Cheng, A Furbach, S Sartania, M Lenzner, Ch Spielmann and F Krausz, *Opt. Lett.* **24**, 247 (1999)
- [21] D Anderson, *Phys. Rev.* **A27**, 3135 (1983)
- [22] G A Swartzlander, D R Andersen, J J Regan, H Yin and A Kaplan, *Phys. Rev. Lett.* **66** 1583 (1991)
- [23] A W Snyder, L Poladian and D J Mitchell, *Opt. Lett.* **17**, 789 (1992)
- [24] P Di Trapani, W Chinaglia, S Minardi, A Piskarskas and G Valiulis, *Phys. Rev. Lett.* **84** 3843 (2000)
- [25] O Bang, *J. Opt. Soc. Am.* **B14**, 51 (1997)
- [26] T J Alexander, Yu S Kivshar, A V Buryak and R A Sammut, *Phys. Rev.* **E61**, 2042 (2000)
- [27] K Y Kolossovski, A V Buryak and R A Sammut, *Phys. Lett.* **A279**, 355 (2001)
- [28] T Peschel, U Peschel, F Lederer and B A Malomed, *Phys. Rev.* **E55**, 4730 (1997)  
W C K Mak, B A Malomed and P L Chu, *Phys. Rev.* **E58**, 6708 (1998)  
E A Ostrovskaya, Y S Kivshar, D V Skryabin and W J Firth, *Phys. Rev. Lett.* **83**, 296 (1999)  
Z H Musslimani, M Segev, D N Christodoulides and M Soljačić, *Phys. Rev. Lett.* **84**, 1164 (2000)  
J N Malmberg, A H Carlsson, D Anderson, M Lisak, E A Ostrovskaya and Y S Kivshar, *Opt. Lett.* **25**, 643 (2000)  
J J García-Ripoll, V M Pérez-García, E A Ostrovskaya and Y S Kivshar, *Phys. Rev. Lett.* **85**, 82 (2000)
- [29] M Mitchell, M Segev and D N Christodoulides, *Phys. Rev. Lett.* **80**, 4657 (1998)  
T Calmon, C Anastassiou, S Lan, D Kip, Z H Musslimani, M Segev and D Christodoulides, *Opt. Lett.* **25**, 1113 (2000)  
W Krolikowski, E A Ostrovskaya, C Weillnau, M Geisser, G McCarthy, Y S Kivshar, C Denz and B Luther-Davies, *Phys. Rev. Lett.* **85**, 1425 (2000)
- [30] O Bang, Y S Kivshar and A V Buryak, *Opt. Lett.* **22**, 1680 (1997)
- [31] L Torner, *IEEE Phot Tech. Lett.* **11**, 1268 (1999)  
O Bang, C Clausen, P Christiansen and L Torner, *Opt. Lett.* **24**, 1413 (1999)  
J F Corney and O Bang, Modulational stability and dark solitons in periodic quadratic nonlinear media, in *Nonlinear optics: materials, fundamentals and applications*, OSA Technical Digest (Optical Society of America, Washington DC, 2000), pp. 362–364